CHEESA: Chemical Engineering Research Articles
ISSN 2614-8757 (Print), ISSN 2615-2347 (Online)
Homepage: https://e-journal.unipma.ac.id/index.php/cheesa

CHEESA, 9(1), pp 26-40, 2026

Potato Peel Starch Bioplastics Reinforced with Microcrystalline Cellulose, PVA, and Chitosan: Mechanical, Thermal, and Antibacterial Properties

Mochamad Viky Afandy[1)], Andoko[1*)], Riduwan Prasetya[1,2)], Muhammad Faizullah Pasha[1)], Mohammad Sukri bin Mustapa[3)]

[1)]*Universitas Negeri Malang, Department of Mechanical and Industrial Engineering, Faculty of Engineering, Jl Semarang 5, Malang, 65145, Indonesia*
[2)]*Universitas Brawijaya, Department of Mechanical Engineering, Faculty of Engineering, Jl MT Haryono 157, Malang, 65145, Indonesia*
[3)]*Universiti Tun Hussein Onn Malaysia, Department of Mechanics Engineering, Faculty of Mechanical and Manufacturing Engineering, Johor, Malaysia*

*corresponding author: andoko.ft@um.ac.id

Article History

Submitted: 10th April 2026; Revised: 27th May 2026; Accepted: 27th May 2026;
Available online: 05th June 2026; Published Regularly: June 2026

doi: 10.25273/cheesa.v9i1.24438.26-40

Abstract

The increasing accumulation of petroleum-based plastic waste has led to the development of biodegradable packaging materials from renewable agro-industrial resources. Therefore, this study aims to synthesize biodegradable potato peel starch/polyvinyl alcohol (PPS/PVA) blend bioplastic films reinforced with microcrystalline cellulose (MCC) and functionalized with chitosan. Films were prepared through solution casting with varied MCC contents and characterized for density, tensile properties, crystallinity, thermal stability, morphology, antibacterial activity, and biodegradability. The results showed that an increase in MCC improved film compactness, tensile strength, crystallinity, and surface uniformity, showing stronger interfacial interactions within the polymer matrix. FTIR confirmed enhanced hydrogen bonding among starch, PVA, chitosan, and MCC, while thermal analysis showed improved resistance to degradation. The produced films also exhibited antibacterial activity against Staphylococcus aureus and Escherichia coli, with the highest performance observed at higher MCC loading. Despite reinforcement, the products remained biodegradable in soil. These results show the potential of PPS/PVA blend bioplastic films containing PPS waste as sustainable materials for active packaging applications.

Keywords: antibacterial packaging; bioplastics; mechanical reinforcement; microcrystalline cellulose; potato starch

1. Introduction

The global reliance on petrochemical-based plastics has raised serious environmental concerns due to their persistence, non-biodegradability, and contribution to pollution in terrestrial and marine ecosystems. Plastic wastes disrupt wildlife, contaminate food chains, and emit greenhouse gases during production and incineration [1],[2]. Despite increased recycling initiatives, limitations in infrastructure and material heterogeneity limit effective waste management [3]. These challenges have accelerated the search for biodegradable alternatives derived from renewable resources, fostering interest in bioplastics that offer environmental compatibility and reduced carbon footprints [4].

In recent years, bioplastics have emerged as a promising solution due to their biodegradability and potential to use a wide range of biomass sources, including starch, vegetable oils, and lignocellulosic agricultural waste [5],[6]. Among these, starch from agro-industrial waste, such as potato peels, has gained attention due to its abundance and high polysaccharide content [7]. However, native starch films often suffer from low mechanical strength and high-water sensitivity, limiting their application [8],[9]. To address the limitation, the current study used a potato peel starch/polyvinyl alcohol (PPS/PVA) blend matrix reinforced with

This is an open access article under the CC BY license (http://creativecommons.org/licenses/by/4.0/)

microcrystalline cellulose (MCC) and functionalized with chitosan. PPS provides a renewable polysaccharide phase and contributes to biodegradability, while PVA acts as a film-forming co-matrix that improves chain continuity and film integrity. MCC was incorporated as a crystalline reinforcing filler to improve compactness, stress transfer, crystallinity, and thermal resistance [10]. Chitosan was added as a functional biopolymer because its hydroxyl and amino groups can interact with the PPS/PVA/MCC matrix and provide antibacterial activity [11]. The interaction among these components is mainly governed by intermolecular hydrogen bonding between hydroxyl groups of PPS, PVA, and MCC, as well as hydroxyl and amino groups of chitosan, which may improve mechanical, structural, thermal, and antibacterial properties.

Previous studies have developed starch-based bioplastics from potato peel and other agro-industrial residues using plasticizers, chemical treatment, or natural fiber reinforcement to improve their physical, mechanical, and biodegradable properties [12]–[14]. PPS has also been reported as a promising feedstock for bioplastic films because it can be converted into biodegradable materials with acceptable physicomechanical properties [15]. However, these studies commonly focused on starch-based films with limited functional components or single-reinforcement systems. PVA/starch/chitosan films have been explored for active packaging applications [16], but their combination with MCC reinforcement derived from a PPS-based system remains less reported. Starch/PVA blend films are widely developed because PVA improves film-forming ability, compatibility, and mechanical integrity in biodegradable packaging systems [17],[18].

The novelty of the current study is in the formulation of a PPS/PVA/MCC/chitosan film system with systematic MCC variation to bridge mechanical reinforcement, structural modification, biodegradability, and antibacterial functionality in one material platform. In this formulation, PVA was not only used as a plasticizing component but also as a co-matrix to improve film continuity, mechanical integrity, and processability. PPS was retained as an agro-waste-derived biodegradable phase, while MCC and chitosan were incorporated to provide structural reinforcement and antibacterial functionality, respectively. A solution casting method was used with varying MCC concentrations to investigate the resulting changes in density, tensile strength, crystallinity, thermal stability, surface morphology, and antimicrobial activity. This study aims to synthesize biodegradable films using PPS as a renewable polysaccharide phase and PVA as the dominant film-forming matrix. The results are expected to offer insights into optimizing bioplastic formulations for sustainable, functional packaging applications.

2. Research Methods

2.1 Tools and Materials

Potato peels were obtained from local potato waste (*Solanum tuberosum* L.) in East Java, Indonesia. MCC (particle size 20 µm), glacial acetic acid, hydrogen peroxide (H_2O_2), glycerol, and sodium hydroxide (NaOH) were purchased from Sigma-Aldrich. PVA and shrimp shell chitosan with a degree of deacetylation ≥ 75% were obtained from HiMedia Laboratories.

Film characterization was carried out using a universal testing machine (UTM, Instron 5567) for tensile analysis, scanning electron microscopy (SEM, JEOL JSM-6510LA) for surface morphology observation, X-ray diffraction (XRD, Bruker D8 Advance) for crystallinity analysis, Fourier transform infrared spectroscopy (FTIR, PerkinElmer Spectrum Two) for functional group identification, and thermogravimetric analysis (TGA, Q500 Thermogravimetry, TA Instruments, USA) for thermal stability evaluation. Antibacterial inhibition zones were measured using a digital calliper (Mitutoyo).

2.2 Potato Peel Starch (PPS) Preparation

The PPS was conducted as shown in Figure 1(a). The potato peels were thoroughly washed to remove dirt and debris, then sun-dried for 3 days until the moisture content was below 10%. Dried peels were ground into fine powder using a grinder and sieved through a 120-mesh screen to obtain a uniform particle size. The resulting powder was treated with 15% (v/v) sodium hydroxide (NaOH) solution at a starch-to-solution ratio of 1:12 (w/v). The mixture was stirred at 100 °C and 240 rpm for one hour using a magnetic stirrer. Subsequently, it was rinsed with distilled water until a neutral pH was achieved. A bleaching step was carried out where10% (v/v) H_2O_2 was added, and the mixture was stirred for 2 hours to enhance starch purity. Finally, the treated starch was filtered using vacuum filtration and poured into Petri dishes, then dried in an oven at 60 °C for 8 hours to yield the purified PPS powder.

2.3 Bioplastic Fabrication

The bioplastic fabrication process, shown in Figure 1(b), was carried out using the solution casting method with minor modifications from previous starch/PVA blend film studies [17],[18]. Briefly, 5 g of PVA was dissolved in 100 mL of distilled water and heated at 80 °C until fully dissolved. Once a homogeneous solution was obtained, 1 g of PPS was added and stirred until well mixed. Meanwhile, 1 g of chitosan was dissolved separately in 10 mL of acetic acid and then added to the PPS/PVA mixture. The fixed PPS:PVA:chitosan ratio was selected to provide a continuous film-forming matrix, maintain PPS as a renewable biodegradable starch phase, and keep chitosan as a constant antibacterial component. MCC was subsequently incorporated according to the variations listed in Table 1. Subsequently, 1 mL of glycerol was added as a plasticizer. The complete mixture was stirred continuously for 30 minutes to ensure that all components were uniformly blended. After a homogeneous mixture was obtained, the same casting volume was poured into Petri dishes with the same diameter and dried in an oven at 45 °C for 16 hours to form bioplastic films. In addition, film thickness was controlled by maintaining the same casting volume, mold diameter, and drying conditions for all formulations. The thickness of each film was measured at 5 different points using a digital micrometer, and the average value was used for further characterization.

Table 1. Variation of microcrystalline cellulose (MCC) in biodegradable film potato peel starch/polyvinyl alcohol (PPS/PVA)

Sample	PPS (g)	PVA (g)	Chitosan (g)	MCC (g)
C0	1	5	1	0
C1	1	5	1	1
C1.5	1	5	1	1.5
C2	1	5	1	2

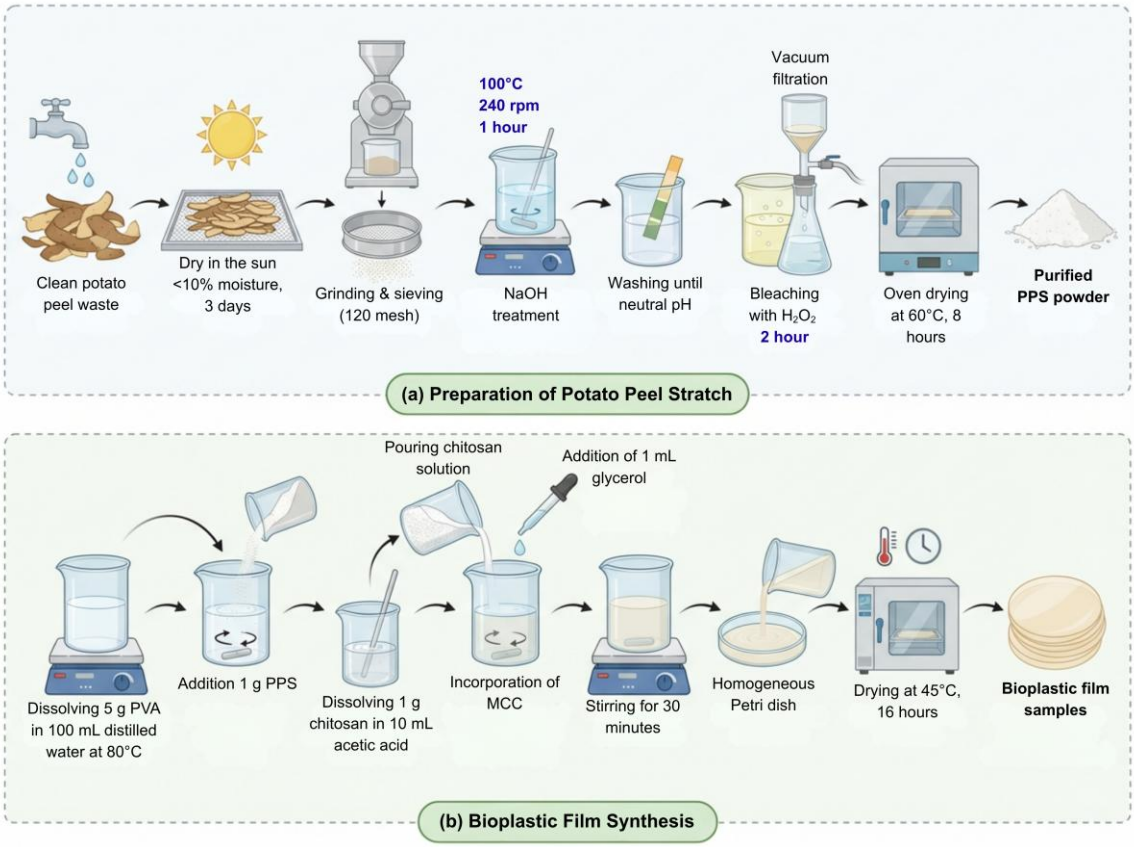

Figure 1. (a) Potato peel starch (PPS) preparation process, (b) bioplastic fabrication process (Generate with AI and substantially modified with Canva)

2.4 Characterization of Bioplastics Films

2.4.1 Density

The density of the films was determined by measuring the sample mass and volume, as calculated using Equation 1. ρ is the density of the bioplastic films (g/cm^3), m is the sample mass (g), and V is the sample volume (cm^3). The sample volume was calculated from the measured length, width, and thickness of the films.

$$\rho = \frac{m}{V} \quad \text{.....(Equation 1)}$$

2.4.2 Mechanical Properties

The mechanical properties of the films were tested according to ASTM D882, and the film specimens were cut into rectangular strips with dimensions of 50 mm × 10 mm. The thickness of each specimen was measured using a digital micrometer before testing and used to calculate the initial cross-sectional area. The test was conducted at a crosshead speed of 10 mm/min and an initial gauge length of 50 mm. Each sample was tested 3 times to obtain the average tensile strength and elongation at break.

Tensile strength and elongation at break were calculated using Equations 2 and 3, respectively. σ is the tensile strength (MPa), F_{max} is the maximum tensile force (N), and A_0 is the initial cross-sectional area of the film (mm^2), calculated from the film width and thickness. Meanwhile, ε is the elongation at break (%), ΔL is the extension at break (mm), and L_0 is the initial gauge length (mm).

$$\sigma = \frac{F_{max}}{A_0} \quad \text{.....(Equation 2)}$$

$$\varepsilon = \frac{\Delta L}{L_0} \times 100\% \quad \text{.....(Equation 3)}$$

2.4.3 Degradation

Degradation testing was carried out using the soil burial method following ASTM D5988. Bioplastic films were buried in soil at room temperature and observed on days 0, 7, 14, and 21 by recording weight loss as an indicator of degradation. Each degradation test was performed in triplicate.

2.4.4 Physical Appearance

Visual changes on the film surface were observed during the soil burial period. The focus of observation included cracking, discoloration, surface damage, and structural disintegration. Documentation was carried out photographically at 0 to 21-day intervals.

2.4.5 Morphology

The surface morphology of the bioplastic films was observed with magnifications of ×4000 and ×1800 to evaluate the initial morphology of the films after fabrication. Before observation, the samples were coated with gold through a sputter-coating process and observed at an acceleration voltage of 15 kV.

2.4.6 Crystallinity Index

The crystalline structure was analyzed with a Cu Kα radiation source. Measurements were taken at a 2θ angle range of 5 to 50° with a scan rate of 1°/minute. The diffraction pattern was used to calculate the crystallinity index and analyze structural changes due to variations in MCC concentration. Equation 4 was used to calculate the crystal index of the bioplastic sample [14].

$$Crl\ (\%) = \frac{Area\ of\ all\ crystal\ peaks}{Area\ all\ amorf\ crystal} \quad \text{...(Equation 4)}$$

2.4.7 Functional Group

Functional groups were observed in the wavelength range of 4000–400 cm^{-1} with a resolution of 4 cm^{-1}. Spectrum data were used to identify functional group interactions and hydrogen bonds between starch, chitosan, and PVA.

2.4.8 Thermal Degradation

Thermal stability was evaluated by heating the samples from 30 °C to 600 °C at a heating rate of 10 °C/minute under a nitrogen atmosphere. The resulting mass loss profile was used to analyze the thermal degradation of the bioplastic films.

2.4.9 Antibacterial Test

Antibacterial activity was evaluated against *Staphylococcus aureus* and *Escherichia coli* using the disk diffusion method on Mueller–Hinton agar based on CLSI M02. The bacterial suspension was adjusted to a 0.5 McFarland standard. Bioplastic films were cut into 6 mm diameter disks and placed on the inoculated agar surface. Chloramphenicol and sterile blank disks were used as positive and negative controls, respectively. The plates were incubated at 37 °C for 24 hours, and the inhibition zone diameter was subsequently measured. Each antibacterial test was performed in triplicate, and the results were

reported as mean ± standard deviation (SD). Statistical significance among formulations was analyzed using one-way analysis of variance (ANOVA) followed by Tukey's post hoc test using Minitab Statistical Software version 20 (Minitab LCC, State College, PA, USA) at a significance level of $p < 0.05$.

3. Results and Discussion

3.1 Density of Bioplastic Films

Density is an important physical parameter for evaluating the compactness and packing quality of PPS/PVA blend bioplastic films after MCC incorporation. As presented in Figure 2, the density of bioplastic films increased progressively with higher concentrations of MCC. The control sample (C0) without MCC exhibited the lowest density, while the sample containing 2 g of MCC (C2) achieved the highest value. This trend suggested a strong correlation between the amount of MCC and the compactness of the resulting bioplastic matrix, confirming that MCC significantly influenced the structural density of the films.

The observed increase in density with MCC addition reflected the dual role of MCC as both a structural filler and a matrix densifier. MCC particles occupied microvoids within the PPS/PVA/chitosan blend matrix, promoting tighter packing and reducing free volume, which led to a denser composite structure [12],[19]. Moreover, the high intrinsic density of MCC contributed directly to the overall mass-to-volume ratio of the films [20],[21]. Uniform dispersion of MCC throughout the matrix enhanced filler-matrix interactions, forming hydrogen bonds that further reinforced the structure and minimized porosity. These combined effects led to more compact and structurally cohesive bioplastic films, which were beneficial for applications requiring dimensional stability and improved mechanical performance.

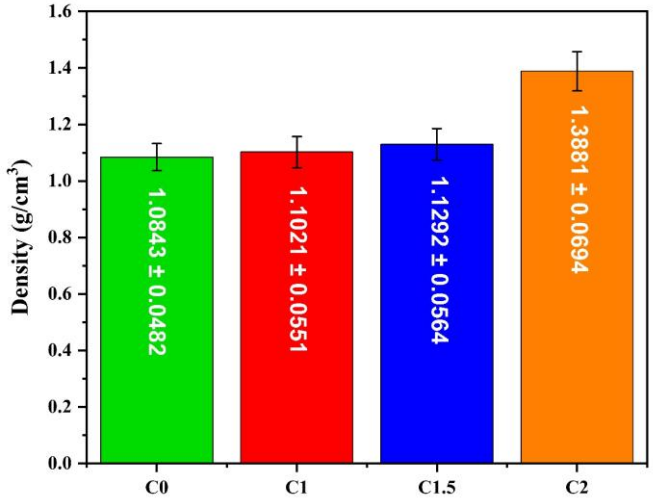

Figure 2. Density of potato peel starch/polyvinyl alcohol/microcrystalline cellulose/chitosan (PPS/PVA/MCC/chitosan) bioplastic films at different microcrystalline cellulose (MCC) loadings: C0 (0 g), C1 (1 g), C1.5 (1.5 g), and C2 (2 g)

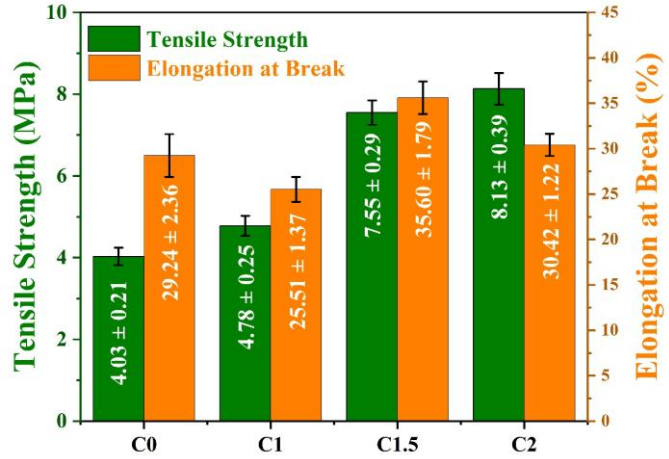

Figure 3. Tensile strength and elongation pat break properties of potato peel starch/polyvinyl alcohol/microcrystalline cellulose/chitosan (PPS/PVA/MCC/chitosan) bioplastic films at different microcrystalline cellulose (MCC) loadings: C0 (0 g), C1 (1 g), C1.5 (1.5 g), and C2 (2 g)

3.2 Mechanical Properties of Bioplastic Films

As shown in Figure 3, the incorporation of MCC significantly influenced the tensile properties of PPS/PVA blend bioplastic films. A consistent improvement in tensile strength was observed with increasing MCC concentrations. The value increased steadily from the control sample (C0) to the highest value at 2 g MCC (C2). However, the elongation at break showed a fluctuating pattern, with the lowest value recorded at C1 and a notable increase at C1.5, followed by a slight decrease at C2. These results showed that MCC had a reinforcing effect on tensile strength, while its impact on flexibility was more complex.

The enhancement in tensile strength could be attributed to the reinforcing role of MCC and the continuous PPS/PVA matrix [22],[23]. Considering the higher amount of PVA in the formulation, PVA played a dominant role in film formation, chain continuity, and load-bearing behavior. Previous starch or PVA studies reported that PVA contributed to film-forming ability, mechanical strength, compatibility, and processability, while starch improved renewability and biodegradation tendency [17],[18],[24].

In this study, the non-linear behavior in elongation at break suggested that while moderate MCC levels enhanced both strength and flexibility, higher concentrations induced particle agglomeration. This agglomeration disrupted matrix homogeneity and introduced stress concentration zones, which hindered polymer chain mobility and reduced ductility [25]. Furthermore, the increase in crystallinity associated with higher MCC levels contributed to film stiffness but compromised flexibility, showing a trade-off between mechanical reinforcement and elongation capacity. These results suggested that an optimal MCC concentration was critical to achieving balanced mechanical performance in bioplastic formulations.

3.3 Biodegradability of Bioplastic Films

Figure 4 showed the weight loss behavior of PPS/PVA blend bioplastic films during the 21-day soil burial period. All formulations exhibited progressive weight loss, confirming their biodegradability. C0 and C2 had the most extensive degradation by the end of the observation period, both reaching comparable mass losses. However, C1 showed a sharp decline in mass during the first week, followed by minimal changes, suggesting early-stage degradation after stabilization. C1.5 presented a more delayed but continuous degradation profile, with a significant increase occurring during the latter half of the test. C2 initially resisted degradation but underwent a rapid breakdown between days 14 and 21, eventually equalling the degradation level of the MCC-free control sample.

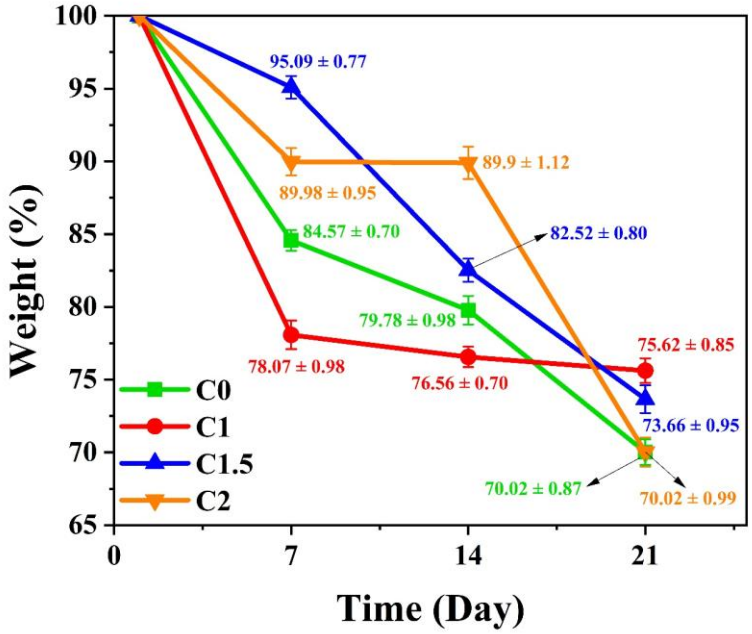

Figure 4. Weight loss behavior of potato peel starch/polyvinyl alcohol/microcrystalline cellulose/chitosan (PPS/PVA/MCC/chitosan) bioplastic films during 21-day soil burial degradation at different microcrystalline cellulose (MCC) loadings: C0 (0 g), C1 (1 g), C1.5 (1.5 g), and C2 (2 g)

The degradation behavior of the bioplastics reflected the dual role of MCC in influencing biodegradability. At lower concentrations, MCC enhanced microbial degradation due to its hygroscopic nature, which facilitated water uptake and microbial colonization [10],[26]. However, as MCC concentration increased, its crystalline structure became more dominant, potentially reducing biodegradability by creating a more stable, less accessible matrix resistant to enzymatic attack. A comparable effect was reported in starch-based systems containing PVA and chitosan, where stronger intermolecular interactions reduced the biodegradation rate but did not eliminate the material's overall biodegradability [11]. This trade-off was evident in the delayed degradation of C2, which initially resisted breakdown but later succumbed, possibly due to surface erosion or structural fatigue. Variations in environmental factors such as moisture and temperature influenced microbial activity and degradation kinetics [27],[28]. These results emphasized the importance of balancing structural reinforcement and degradability in bioplastic design to ensure both performance and environmental compatibility.

3.4 Physical Appearance of Bioplastic Films

Figure 5 provided a visual record of surface changes across all bioplastic samples during the 21-day soil burial period. The physical changes were closely related to the quantitative weight loss results shown in Figure 4. Samples with more pronounced discoloration, surface spots, deformation, and structural collapse showed lower final weight retention, showing higher degradation. This relationship was evident in C0 and C2, which showed the lowest remaining weight after 21 days, both around 70.02%, and also showed more visible surface deterioration. However, C1 and C1.5 retained higher final weights of 75.62% and 73.66%, respectively, which corresponded to their relatively more intact visual appearance. The physical appearance changes supported the quantitative degradation results, where visible surface damage reflected progressive weight loss during soil burial.

The morphological alterations observed were characteristic of microbial degradation activity, where cracks and surface ruptures facilitated deeper microbial access to the PPS/PVA/chitosan matrix. The incorporation of MCC affected this process in complex ways. While it could increase elasticity and reduce early fragmentation [29], higher concentrations enhanced mechanical integrity and water resistance, thereby slowing down microbial penetration and degradation [30]. This interplay explained the delayed but eventual degradation of C2. Furthermore, visible biological indicators, such as fungal growth and biomolecule deposition, corroborate ongoing microbial activity despite the protective effects of MCC [31]. The results emphasized the dual role of reinforcement agents in both structural enhancement and biodegradation modulation.

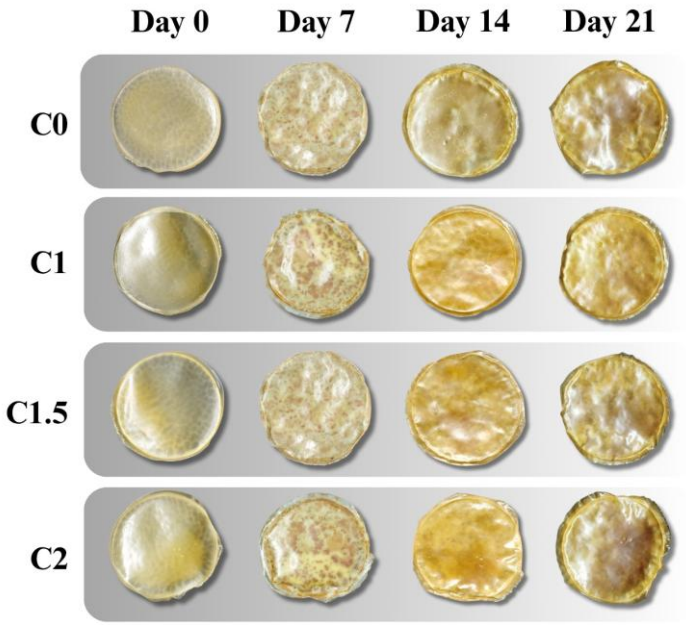

Figure 5. Physical appearance changes of potato peel starch/polyvinyl alcohol/microcrystalline cellulose/chitosan (PPS/PVA/MCC/chitosan) bioplastic films during 21-day soil burial degradation at different microcrystalline cellulose (MCC) loadings: C0 (0 g), C1 (1 g), C1.5 (1.5 g), and C2 (2 g)

3.5 Thermal Degradation of Bioplastic Films

Figures 6a and 6b showed that all bioplastic samples underwent 3 distinct stages of thermal decomposition, with the primary mass loss occurring between 260 and 310 °C. Among the tested samples, C1.5 exhibited the most notable thermal stability, as shown by its lower TGA mass loss, broader and shallower DTG peak, and higher residual mass after thermal treatment. The value reported in Table 2 represented mass loss during TGA. Therefore, a lower value showed less thermal decomposition and better thermal resistance.

The enhancement in thermal performance observed in MCC-containing bioplastics could be attributed to the reinforcement effect of MCC, which increased the thermal resistance of the polymer matrix. This was evidenced by the shift in initial degradation and peak decomposition temperatures, as well as increased temperatures for 10% and 50% weight loss [32]. The formation of strong hydrogen bonds between MCC and PPS/PVA/chitosan matrix components contributed to higher thermal stability by creating a more rigid and cohesive composite network. Furthermore, the improved crystallinity due to MCC integration further supported resistance to thermal breakdown [33]. The formation of a more stable residue in C1.5 suggested that moderate MCC loading produced a more effective thermal barrier than excessive MCC addition. These results emphasized the suitability of MCC-reinforced bioplastics for applications requiring greater thermal endurance, such as food packaging exposed to elevated processing or storage temperatures.

3.6 Morphology of Bioplastic Films

Figure 7 micrographs showed progressive improvements in the surface and internal structure of bioplastics with increasing MCC content. The control sample (C0) exhibited a rough, cracked, and highly inhomogeneous surface, indicative of poor structural integrity. In sample C1, the presence of MCC began to reduce surface imperfections, but visible cracks and uneven layering persisted. A more noticeable improvement was observed in C1.5, where the surface appeared smoother, and cracks were reduced, but with a porous cross-section. The most uniform morphology was observed in sample C2, which showed a dense, crack-free surface and a relatively homogeneous internal structure. No severe MCC agglomeration was clearly detected at the observed SEM magnification, although localized filler-rich regions or stronger filler–matrix interactions still occurred and contributed to the increased stiffness of the films.

The morphological improvements observed through SEM analysis affirmed the role of MCC in enhancing the microstructure of PPS/PVA blend bioplastic films. MCC acted as a structural filler that filled voids and facilitated stronger hydrogen bonding within the matrix, contributing to smoother and more cohesive films [34]. These structural refinements were crucial, directly correlating with enhanced mechanical strength and thermal resistance by reducing defect sites that could initiate failure under stress or heat. Moreover, the denser microstructure in higher MCC samples suggested reduced porosity and fewer structural defects, which supported better dimensional stability and durability.

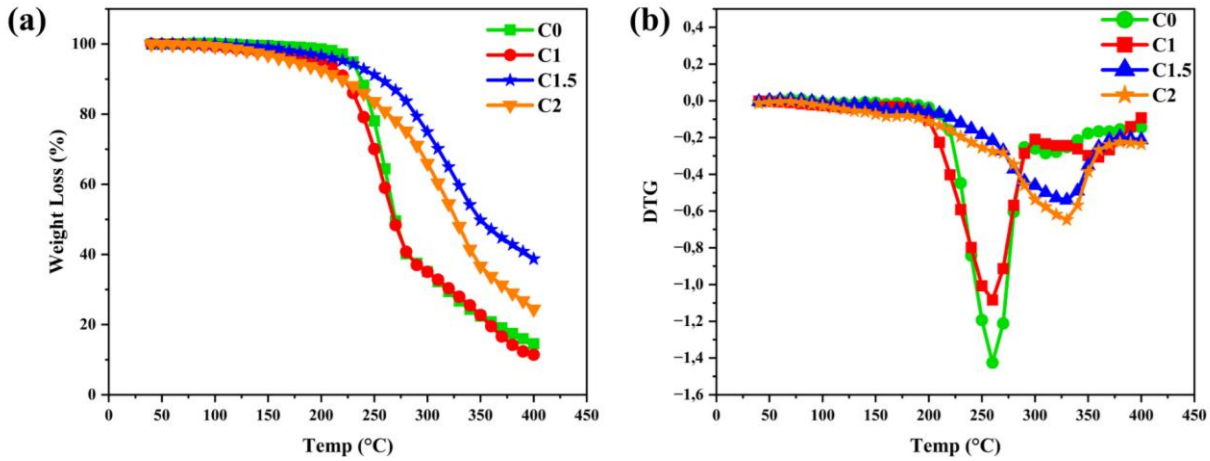

Figure 6. Thermal degradation profiles of potato peel starch/polyvinyl alcohol/microcrystalline cellulose/chitosan (PPS/PVA/MCC/chitosan) bioplastic films at different microcrystalline cellulose (MCC): C0 (0 g), C1 (1 g), C1.5 (1.5 g), and C2 (2 g), showing (a) thermogravimetric analysis (TGA) and (b) derivative thermogravimetry (DTG) curves

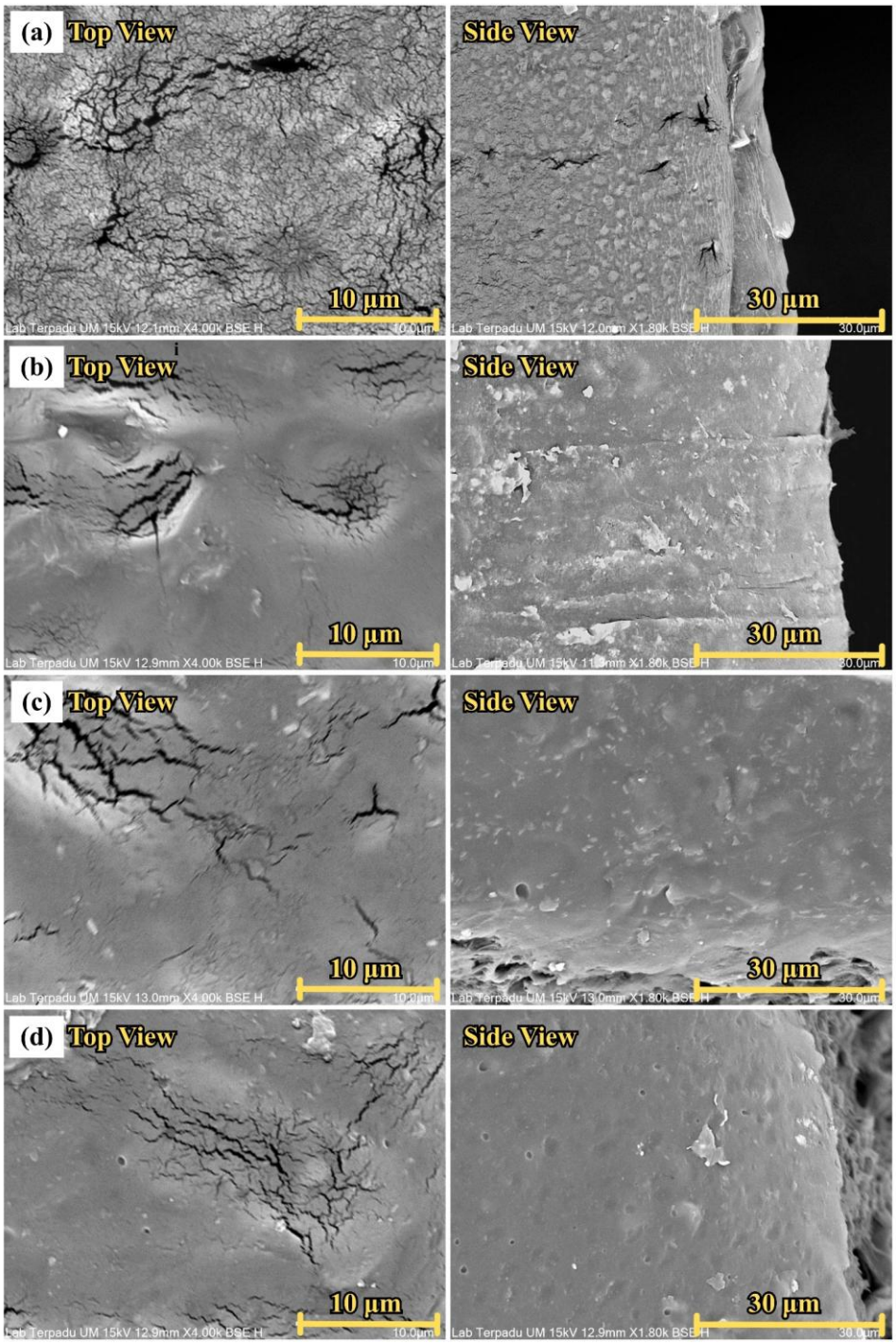

Figure 7. Surface and cross-sectional micrographs of potato peel starch/polyvinyl alcohol/microcrystalline cellulose/chitosan (PPS/PVA/MCC/chitosan) bioplastic films before soil burial degradation at different microcrystalline cellulose (MCC) loadings: (a) C0 (0 g), (b) C1 (1 g), (c) C1.5 (1.5 g), and (d) C2 (2 g)

3.7 Crystallinity Index of Bioplastic Films

As shown in Figure 8, the dominant XRD peaks around 2θ = 19–23° must not be assigned to a single component. In the PPS/PVA/MCC/chitosan system, this region represented overlapping diffraction from the semi-crystalline PVA phase, as reported in starch/PVA blend films [17],[18]. The PPS phase could also contribute to the diffraction response because starch-based bioplastic films generally exhibited semi-crystalline polysaccharide structures [15]. The sharper and more intense peaks observed with increasing MCC loading showed the contribution of crystalline cellulose domains from MCC, which promoted molecular ordering in the blend matrix [10],[23]. The diffraction peak intensity and sharpness progressively increased from C0 to

C2, showing an enhancement in structural order. Sample C2 showed the most defined and symmetrical peaks, which were consistent with the highest crystallinity index recorded. This trend confirmed that increasing MCC content significantly increased the internal crystalline arrangement of the bioplastics.

The observed increase in crystallinity index with higher MCC concentrations reflected the role of MCC in promoting molecular alignment within the bioplastic matrix. MCC served as a nucleating agent that facilitated orderly polymer chain packing, thereby reinforcing the internal structure [10],[23]. This elevated crystallinity was strongly associated with improvements in key material properties, including enhanced tensile strength due to tighter intermolecular interactions and increased thermal stability through delayed chain mobility and decomposition [32],[35]. In this study, higher crystallinity and compact morphology reduced free volume and diffusion pathways. The increased crystallinity index influenced the biodegradation behavior by forming a more ordered and compact structure that could limit water diffusion and microbial access to the polymer chains [27],[28]. This effect explained why MCC-containing films, specifically C1 and C1.5, showed higher final weight retention than the MCC-free control. However, crystallinity was not the only factor controlling biodegradation, because soil burial degradation was affected by hydrophilicity, surface defects, filler distribution, matrix composition, and microbial activity [30],[31]. Although C2 showed the highest crystallinity index, it also exhibited relatively high weight loss after soil burial. This behavior was related to the high MCC loading, which increased crystalline order but also introduced more hydroxyl-rich cellulose domains and interfacial pathways that facilitated water penetration and microbial access during soil burial [27],[28],[31]. Therefore, the degradation behavior of C2 reflected the combined effects of crystalline order, hydrophilicity, matrix composition, and filler–matrix interactions rather than crystallinity alone.

Table 2. Summary of thermal mass loss and crystallinity index of potato peel starch/polyvinyl alcohol/microcrystalline cellulose/chitosan (PPS/PVA/MCC/chitosan) bioplastic films at different microcrystalline cellulose (MCC) loadings: C0 (0 g), C1 (1 g), C1.5 (1.5 g), and C2 (2 g)

Sample	TGA Mass Loss (%)	Crystallinity Index (%)
C0	85.45	72.39
C1	88.58	79.49
C1.5	61.29	80.98
C2	75.57	89.92

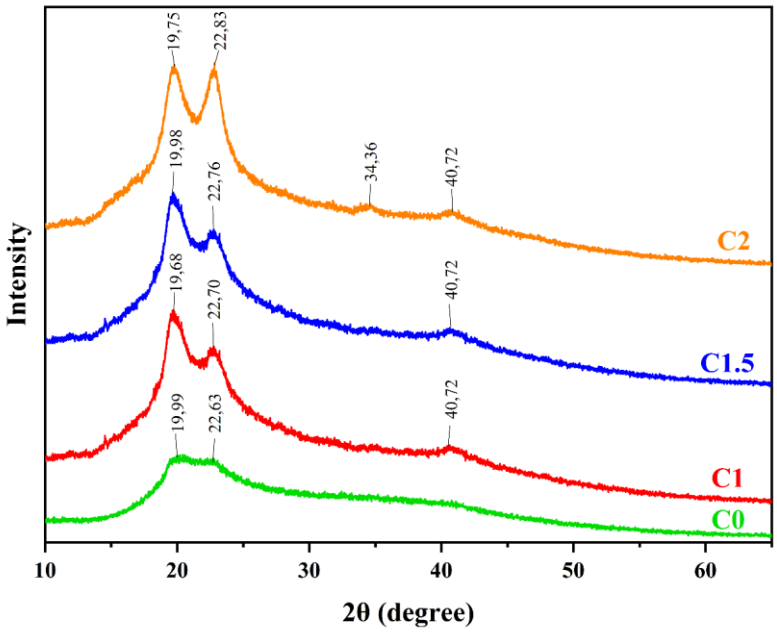

Figure 8. XRD patterns of potato peel starch/polyvinyl alcohol/microcrystalline cellulose/chitosan (PPS/PVA/MCC/chitosan) bioplastic films at different microcrystalline cellulose (MCC) loadings: C0 (0 g), C1 (1 g), C1.5 (1.5 g), and C2 (2 g)

3.8 Functional Group of Bioplastic Films

The FTIR spectra shown in Figure 9 showed characteristic absorption bands corresponding to key functional groups present in the PPS/PVA/MCC/chitosan matrix. Broad absorption around 3665–3677 cm^{-1} showed O–H stretching vibrations from hydroxyl groups found in starch, PVA, and MCC [36]. Aliphatic C–H stretching, observed in the 2947–2959 cm^{-1} range, was attributed to glucose chains in the polysaccharide components [16]. The presence of carbonyl (C=O) groups was confirmed by bands around 1702–1714 cm^{-1}, suggesting contributions from modified PVA and oxidized MCC [35]. Furthermore, CH_2 deformation bands appeared between 1473–1486 cm^{-1}, and strong signals in the 1122–1151 cm^{-1} region reflected glycosidic C–O–C and ether C–O bonding patterns [35].

The FTIR spectra showed notable shifts and intensity changes in absorption bands with increasing MCC concentration, showing enhanced molecular interactions within the PPS/PVA/chitosan matrix. The broad O–H stretching region showed hydrogen bonding among hydroxyl groups of PPS, PVA, and MCC, while the amino and hydroxyl groups of chitosan further contributed to matrix cohesion. No new dominant absorption peak was observed, suggesting that the interaction mechanism was mainly associated with intermolecular hydrogen bonding and filler–matrix adhesion rather than the formation of new covalent bonds. These interactions supported improved compactness, crystallinity, tensile strength, and thermal stability of the bioplastic films [10],[35]. The slight shift and variation in C–H and C=O bands confirmed secondary hydrogen bonding and polymer chain interactions [37]. The molecular linkages suggested good compatibility among components, leading to a more integrated network. In addition, ether-related bands (C–O–C) in the fingerprint region (1192–950 cm^{-1}) supported the formation of glycosidic linkages and interchain connectivity [10]. Collectively, the FTIR analysis provided evidence of strong interfacial bonding and enhanced chemical compatibility, which were essential for producing bioplastics with improved physical and functional stability.

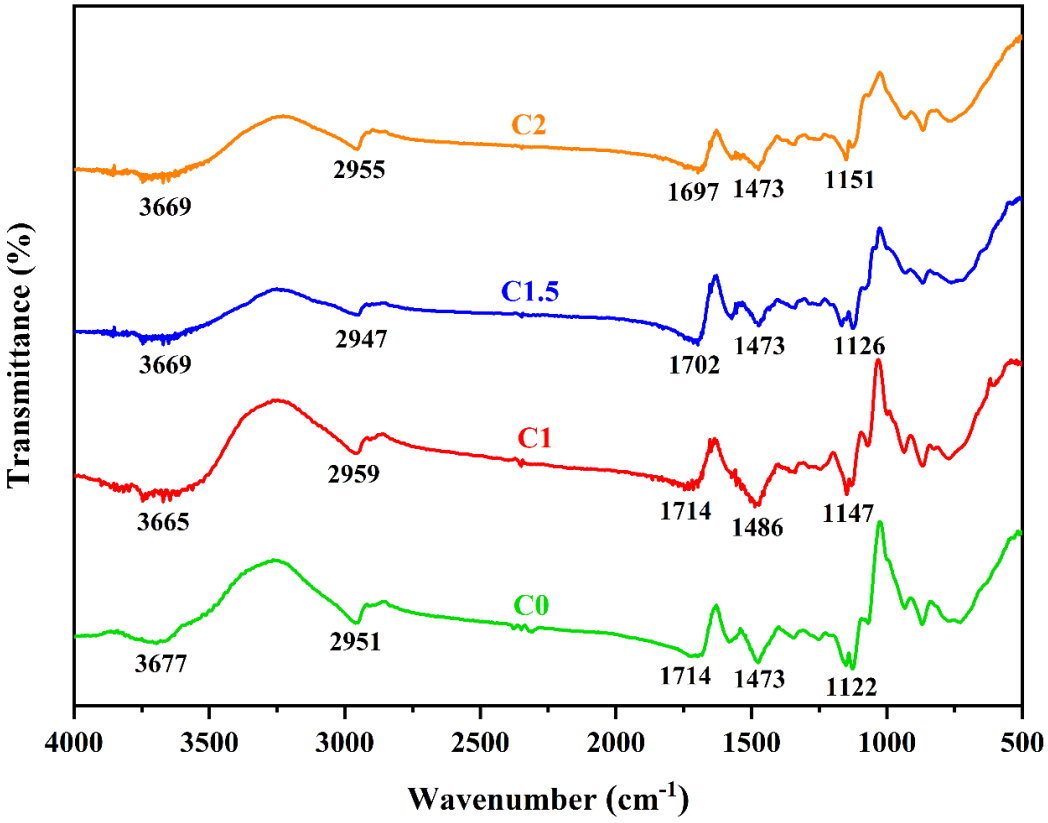

Figure 9. FTIR spectra of potato peel starch/polyvinyl alcohol/microcrystalline cellulose/chitosan (PPS/PVA/MCC/chitosan) bioplastic films at different microcrystalline cellulose (MCC) loadings: C0 (0 g), C1 (1 g), C1.5 (1.5 g), and C2 (2 g)

Table 3. Antibacterial inhibition zone of potato peel starch/polyvinyl alcohol/microcrystalline cellulose/chitosan (PPS/PVA/MCC/chitosan) bioplastic films at different microcrystalline cellulose (MCC) loadings: C0 (0 g), C1 (1 g), C1.5 (1.5 g), and C2 (2 g) against *Staphylococcus aureus* and *Escherichia coli*

Sample	Inhibition Zone (mm)	
	Staphylococcus aureus	***Escherichia coli***
C0	4.98 ± 0.49^{c}	5.98 ± 0.53^{b}
C1	9.70 ± 0.77^{b}	8.60 ± 0.56^{a}
C1.5	4.26 ± 0.30^{c}	3.85 ± 0.50^{c}
C2	15.70 ± 0.73^{a}	7.59 ± 0.64^{a}
Positive control (Chloraphenicol)	22.32	21.85
Negative control (Aquadest)	NI	NI

3.9 Antibacterial Properties of Bioplastic Films

Antibacterial performance was evaluated to determine the functional potential of PPS/PVA/MCC/chitosan films for active packaging applications. The antibacterial activity results, presented in Table 3, showed that the inhibition zones varied among the formulations rather than increasing linearly with MCC concentration. This non-linear trend was particularly evident for *Escherichia coli*, where C1 showed a higher inhibition zone than C2 despite a higher MCC loading. Sample C1 showed higher antibacterial activity than C1.5 against both *Staphylococcus aureus* and *E. coli*. This decrease at C1.5 could be associated with the structural effect of MCC on the PPS/PVA/chitosan matrix. At moderate MCC loading, stronger hydrogen bonding and a denser matrix restricted the exposure or diffusion of chitosan amino groups toward the agar medium, resulting in a smaller inhibition zone [35]. Therefore, the lower antibacterial activity of C1.5 compared with C1 was not attributed to reduced chitosan content, because chitosan was kept constant, but rather to differences in matrix compactness, component distribution, and accessibility of antibacterial functional groups.

Positive and negative controls were used to validate the antibacterial assay and were not included in the statistical grouping, where NI showed no inhibition. The positive control, chloramphenicol, produced clear inhibition zones of 22.32 mm against *S. aureus* and 21.85 mm against *E. coli*, confirming the validity of the disk diffusion assay. Meanwhile, the negative control, aquadest, showed no inhibition zone, showing that the antibacterial response observed in the film samples was not caused by the solvent or testing medium. Table 3 showed the results of multiple comparisons using Tukey's post hoc test following one-way ANOVA. Values sharing at least an identical superscript letter within the same bacterial group were not significantly different, while those with different superscript letters showed statistically significant differences at $p < 0.05$.

The antibacterial activity of the films was mainly associated with the presence of chitosan in the PPS/PVA/MCC matrix. Chitosan contributed to antimicrobial action through its cationic amino groups, which interacted electrostatically with negatively charged bacterial cell surfaces and disrupted membrane integrity [37]. MCC was not considered a primary antibacterial agent in this study, but affected antibacterial performance indirectly through changes in matrix compactness, chitosan distribution, and accessibility of functional groups. Therefore, the antibacterial response occurred due to a combined effect of chitosan activity and MCC-induced modification of the film matrix structure, rather than as a direct antibacterial activity of MCC [38]. These results showed the formulation's suitability for active packaging applications, particularly in extending shelf life and maintaining hygiene standards in food and biomedical products.

Statistical analysis confirmed significant differences in inhibition zones among formulations for both *S. aureus* and *E. coli* ($p < 0.001$). For *S. aureus*, C2 showed the highest inhibition zone and was significantly different from others. For *E. coli*, C1 and C2 were not significantly different from each other, but both showed significantly higher inhibition zones than C0 and C1.5.

4. Conclusion

In conclusion, this study aimed to develop biodegradable bioplastics from PPS reinforced with MCC, plasticized with polyvinyl alcohol, and enhanced with chitosan for antibacterial functionality. The results showed that increasing MCC concentration significantly improved bioplastic mechanical strength, thermal stability, structural integrity, and antibacterial performance, with the formulation containing 2 g MCC showing the most balanced and superior properties. The

addition of MCC enhanced crystallinity and film morphology while maintaining biodegradability in soil, confirming the material's environmental compatibility. However, variations in elongation at break and degradation rate at higher filler levels showed a trade-off between reinforcement and flexibility, suggesting the need for careful optimization. Future studies are advised to compare density, mechanical properties, and thermal stability before and after soil burial, as well as evaluate long-term migration and safety aspects for food-contact applications. These results support the potential of agricultural waste-based bioplastics as viable alternatives to conventional plastics in active and sustainable packaging solutions.

AI Usage Statements

During the preparation of this manuscript, the authors used AI STEM Visualizer (GPAI) solely to generate the initial graphical elements of Figure 1. All AI-generated outputs were critically reviewed and substantially modified by the authors using Canva before inclusion in the manuscript. No AI tools were used for manuscript writing, data analysis, interpretation of results, or conclusion development. The authors take full responsibility for the integrity and content of this manuscript.

CRediT Authorship Statement

Mochamad Viky Afandy: Conceptualization, Methodology, Investigation, Formal analysis, Writing – Original Draft. **Andoko:** Supervision, Project administration, Funding acquisition, Writing – review & editing. **Riduwan Prasetya:** Validation, Visualization, Writing – review & editing. **Muhammad Faizullah Pasha:** Investigation, Resources, Data curation. **Mohammad Sukri bin Mustapa:** Supervision, Validation, Resources, Writing – review & editing.

Declaration of competing interest

The authors declare there is no conflict of interest

Acknowledgments

This study was funded by PNBP 2025 Universitas Negeri Malang with contract number 24.2.873/UN32.14.1/LT/2025.

References

[1] Dimassi, S. N., Hahladakis, J. N., Yahia, M. N. D., Ahmad, M. I., Sayadi, S., & Al-Ghouti, M. A. (2022). Degradation-fragmentation of marine plastic waste and their environmental implications: A critical review. *Arabian Journal of Chemistry*, 15(11), 104262. doi: 10.1016/j.arabjc.2022.104262

[2] Kumar, M., Bolan, S., Padhye, L. P., Konarova, M., Foong, S. Y., Lam, S. S., … Bolan, N. (2023). Retrieving back plastic wastes for conversion to value added petrochemicals: opportunities, challenges and outlooks. *Applied Energy*, 345, 121307. doi: 10.1016/j.apenergy.2023.121307

[3] Bishop, G., Styles, D., & Lens, P. N. L. (2021). Environmental performance comparison of bioplastics and petrochemical plastics: A review of life cycle assessment (LCA) methodological decisions. *Resources, Conservation and Recycling*, 168, 105451. doi: 10.1016/j.resconrec.2021.105451

[4] Ali, Z., Abdullah, M., Yasin, M. T., Amanat, K., Ahmad, K., Ahmed, I., … Khan, J. (2024). Organic waste-to-bioplastics: Conversion with eco-friendly technologies and approaches for sustainable environment. *Environmental Research*, 244, 117949. doi: 10.1016/j.envres.2023.117949

[5] Costa, A., Encarnação, T., Tavares, R., Todo Bom, T., & Mateus, A. (2023). Bioplastics: Innovation for Green Transition. *Polymers*, 15(3), 517. doi: 10.3390/polym15030517

[6] Nanda, S., Patra, B. R., Patel, R., Bakos, J., & Dalai, A. K. (2022). Innovations in applications and prospects of bioplastics and biopolymers: a review. *Environmental Chemistry Letters*, 20(1), 379–395. doi: 10.1007/s10311-021-01334-4

[7] Hamin, S. H., Sayid Abdullah, S. H. Y., Lananan, F., Abdul Hamid, S. H., Kasan, N. A., Mohamed, N. N., & Endut, A. (2023). Effect of chemical treatment on the structural, thermal, and mechanical properties of sugarcane bagasse as filler for starch-based bioplastic. *Journal of Chemical Technology & Biotechnology*, 98(3), 625–632. doi: 10.1002/jctb.7218

[8] Kassim, N. I. A. C., Gunny, A. A. N., Saifuddin, M. N. A. A., Sam, S. T., Ali, F., Jamaluddin, J., … Che Kassim, F. N. (2025). Issues and Challenges of Starch-Based Bioplastics: A Review (pp. 197–207). doi: 10.1007/978-981-96-3785-0_16

[9] Ribba, L., Garcia, N. L., D'Accorso, N., & Goyanes, S. (2017). Disadvantages of Starch-Based Materials, Feasible Alternatives in Order to Overcome These Limitations. In *Starch-Based Materials in Food Packaging* (pp. 37–76). Elsevier. doi: 10.1016/B978-0-12-809439-6.00003-0

[10] Abdullah, A. H. D., Putri, O. D., Fikriyyah, A. K., Nissa, R. C., & Intadiana, S. (2020). Effect of microcrystalline cellulose on characteristics of cassava starch-based bioplastic. *Polymer-Plastics Technology and Materials*, 59(12), 1250–1258. doi: 10.1080/25740881.2020.1738465

[11] Syarifah, N. L., Masriatini, R., Wahyudi, A., Fatimura, M., & Laila Syarifah, N. (2025). Biofoam Cassava Starch and Sugarcane Bagasse Cellulose with the Addition of Polyvinyl Alcohol and Chitosan. *CHEESA: Chemical Engineering Research Articles*, 8(2), 93. doi: 10.25273/cheesa.v8i2.22973.93-102

[12] Arifin, U. F., Adetya, N. P., Pambudi, W., & Ratnaningsih, W. (2022). Quality Evaluation of Bioplastic from Glutinous Rice Starch Reinforced with Bamboo Leaf Powder. *CHEESA: Chemical Engineering Research Articles*, 5(2), 82. doi: 10.25273/cheesa.v5i2.14235.82-91

[13] Bello, T. K., Eze, E. C., Usman, M. S., & Isa, M. T. (2024). Characterization of bioplastics produced from yam and potato peels using hydrochloric and acetic acids. *Biomass Conversion and Biorefinery*, 14(15), 18019–18030. doi: 10.1007/s13399-023-04021-2

[14] Chaffa, T. Y., Meshesha, B. T., Mohammed, S. A., & Jabasingh, S. A. (2024). Production, characterization, and optimization of starch-based biodegradable bioplastic from waste potato (Solanum tuberosum) peel with the reinforcement of false banana (Ensete ventricosum) fiber. *Biomass Conversion and Biorefinery*, 14(21), 27365–27377. doi: 10.1007/s13399-022-03426-9

[15] Sultan, A., Sultan, H., Shahzad, W., Kareem, A., Liaqat, A., Ashraf, Z., … Acevedo, R. (2024). Comparative analysis of physical and mechanical properties of starch based bioplastic derived from the pulp and peel of potatoes. *Journal of the Indian Chemical Society*, 101(10), 101301. doi: 10.1016/j.jics.2024.101301

[16] Momtaz, F., Momtaz, E., Mehrgardi, M. A., Momtaz, M., Narimani, T., & Poursina, F. (2024). Enhanced antibacterial properties of polyvinyl alcohol/starch/chitosan films with NiO–CuO nanoparticles for food packaging. *Scientific Reports*, 14(1), 7356. doi: 10.1038/s41598-024-58210-8

[17] Deng, H., Su, J., Zhang, W., Khan, A., Sani, M. A., Goksen, G., … Rhim, J.-W. (2024). A review of starch/polyvinyl alcohol (PVA) blend film: A potential replacement for traditional plastic-based food packaging film. *International Journal of Biological Macromolecules*, 273, 132926. doi: 10.1016/j.ijbiomac.2024.132926

[18] Ma, N., Dong, W., Qin, D., Dang, C., Xie, S., Wang, Y., … Kumar, R. (2024). Green and renewable thermoplastic polyvinyl alcohol/starch blend film fabricated by melt processing. *International Journal of Biological Macromolecules*, 279, 134866. doi: 10.1016/j.ijbiomac.2024.134866

[19] Khui, P. L. N., Rahman, M. R., & Bakri, M. K. Bin. (2022). Cellulose reinforcement in bioplastic composites. In *Fundamentals and Recent Advances in Nanocomposites Based on Polymers and Nanocellulose* (pp. 143–158). Elsevier. doi: 10.1016/B978-0-323-85771-0.00016-6

[20] Divakaran, D., Sriariyanun, M., Jagadeesan, R., Suyambulingam, I., Sanjay, M. R., & Siengchin, S. (2024). Isolation and characterization of an agro-industrial waste-based novel cellulosic micro fillers from mustard (Brassica juncea) seed oil cake: A waste to wealth approach. *Biomass Conversion and Biorefinery*, 14(18), 22921–22937. doi: 10.1007/s13399-023-04346-y

[21] Sunesh, N. P., Indran, S., Divya, D., & Suchart, S. (2022). Isolation and characterization of novel agrowaste-based cellulosic micro fillers from Borassus flabellifer flower for polymer composite reinforcement. *Polymer Composites*, 43(9), 6476–6488. doi: 10.1002/pc.26960

[22] Nasution, H., Asdita, M., Zoelva, A., Syabina Asraf, F., Atqia Tamanni, D., & Mufidah Lubis, N. (2024). The Effect of Microcrystal Cellulose Filling from Coconut Fiber and Betel Leaf Extract as Antimicrobials on Sago Starch Bioplastic Composite. *E3S Web of Conferences*, 519, 04003. doi: 10.1051/e3sconf/202451904003

[23] Lubis, M., Bangun Harahap, M., Hendra, M., Ginting, S., Sartika, M., & Azmi, H. (2018). Production Of Bioplastic from Avocado Seed Starch Reinforced with Microcrystalline Cellulose from Sugar Palm Fibers. *Journal of Engineering Science and Technology*, 13(2), 381–393.

[24] Shrestha, B., Chapain, K., Shah, S., & Pandit, R. (2023). Starch/ Polyvinyl Alcohol (PVA) Blend Bioplastics: Synthesis and Physicochemical Properties. *Journal of Nepal Chemical Society*, 43(2), 103–109. doi: 10.3126/jncs.v43i2.53349

[25] Faisal, M., Žmirić, M., Kim, N., Bruun, S., Mariniello, L., Famiglietti, M., … Blennow, A. (2023). A Comparison of Cellulose Nanocrystals and Nanofibers as Reinforcements to Amylose-Based Composite Bioplastics. *Coatings*, 13(9), 1573. doi: 10.3390/coatings13091573

[26] Shuprajhaa, T., Paramasivam, S. K., Pushpavalli, S., Anandakumar, Su., & Naik, R. (2025). Influence of additives on the development, mechanical, functional characteristics and biodegradability of banana starch-based bio plastic films. *International Journal of Biological Macromolecules*, 295, 139544. doi: 10.1016/j.ijbiomac.2025.139544

[27] Area, M. R., Montero, B., Rico, M., Barral, L., Bouza, R., & López, J. (2020). Properties and behavior under environmental factors of isosorbide-plasticized starch reinforced with microcrystalline cellulose biocomposites. *International Journal of Biological Macromolecules*, 164, 2028–2037. doi: 10.1016/j.ijbiomac.2020.08.075

[28] Julinová, M., Vaňharová, L., Jurča, M., Minařík, A., Duchek, P., Kavečková, J., … Skácelík, P. (2020). Effect of Different Fillers on the Biodegradation Rate of Thermoplastic Starch in Water and Soil Environments. *Journal of Polymers and the Environment*, 28(2), 566–583. doi: 10.1007/s10924-019-01624-7

[29] Nurhamiyah, Y., Marlina, R., & Syamani, F. A. (2022). Dynamic Mechanical Properties of Acetylated Cassava Starch-Chitosan Based Film, With Addition of Sorghum Micro-Fibrillated Cellulose (pp. 159–169). doi: 10.1007/978-981-19-0308-3_12

[30] Bangar, S. P., Whiteside, W. S., Dunno, K. D., Cavender, G. A., & Dawson, P. (2022). Pearl millet starch-based nanocomposite films reinforced with Kudzu cellulose nanocrystals and essential oil: Effect on functionality and biodegradability. *Food Research International*, 157, 111384. doi: 10.1016/j.foodres.2022.111384

[31] Rumi, S. S., Liyanage, S., & Abidi, N. (2024). Soil burial-induced degradation of cellulose films in a moisture-controlled environment. *Scientific Reports*, 14(1), 6921. doi: 10.1038/s41598-024-57436-w

[32] Olusanya, J. O., Turup Pandurangan, M., & Kanny, K. (2023). Influence of alkali treated cellulose nanoparticles filled starch-based bioplastic films and their effect on thermal and mechanical properties. *Journal of Industrial Textiles*, 53. doi: 10.1177/15280837231198016

[33] Wang, W., Han, L., Zhai, X., Li, Z., Wang, A., Wu, T., & Hou, H. (2021). Etherification of Microcrystalline Cellulose for Application in Starch Films. *Shipin Kexue/Food Science*, 42, 65–71. doi: 10.7506/spkx1002-6630-20200128-283

[34] Żołek-Tryznowska, Z., Bednarczyk, E., Tryznowski, M., & Kobiela, T. (2023). A Comparative Investigation of the Surface Properties of Corn-Starch-Microfibrillated Cellulose Composite Films. *Materials*, 16(9), 3320. doi: 10.3390/ma16093320

[35] Hsiao, K.-Y., Chung, R.-J., Chang, P.-P., & Tsai, T.-H. (2025). Identification of Hydroxyl and Polysiloxane Compounds via Infrared Absorption Spectroscopy with Targeted Noise Analysis. *Polymers*, 17(11), 1533. doi: 10.3390/polym17111533

[36] Khatun, M. A., Sultana, S., Islam, Z., Kabir, M. S., Hossain, M. S., Nur, H. P., & Chowdhury, A. M. S. (2023). Extraction of crystalline nanocellulose (CNC) from date palm mat fibers and its application in the production of nanocomposites with polyvinyl alcohol and polyvinylpyrrolidone blended films. *Results in Engineering*, 17, 101031. doi: 10.1016/j.rineng.2023.101031

[37] Rao, L. S., Naidu, C. D., & Tiwari, S. (2022). Investigation on synthesis, structure and degradability of starch based bioplastics. *Materials Today: Proceedings*, 49, 257–261. doi: 10.1016/j.matpr.2021.01.917

[38] Andoko, A., Prasetya, R., Cakra, B. D., Syah, M. Z., & Santoso, A. (2025). Autoclave-assisted multi-objective optimization of the deacetylation process in chitosan production from shrimp shell waste via response surface methodology. *Results in Engineering*, 27, 106353. doi: 10.1016/j.rineng.2025.106353